

Nonequilibrium Phase Selection during Weld Solidification of Fe-C-Mn-Al Steels[†]

S. S. Babu¹, J. M. Vitek¹, J. W. Elmer², T. A. Palmer² and S. A. David¹

¹Oak Ridge National Laboratory, Oak Ridge, Tennessee 37831-6096, USA

²Lawrence Livermore National Laboratory, Livermore, California 94551-0808, USA

Keywords: Steel, Weld, Solidification, Phase Selection, Time-Resolved X-ray diffraction, modeling, Synchrotron

Abstract

The phase selection phenomenon as a function of interface growth velocity was investigated in an Fe-C-Al-Mn self-shielded flux cored arc weld metal deposit. In this steel, under normal weld cooling conditions, the primary solidification occurs by δ -ferrite formation. With an increase in liquid-solid interface velocity a transition to nonequilibrium austenite solidification was observed. The above phase selection phenomenon was tracked in-situ using a time-resolved X-ray diffraction technique employing Synchrotron radiation. Using the theoretical treatment of dendritic solidification and phase selection maps advanced by Kurz and his co-workers, the microstructure evolution at high weld solidification rates was evaluated.

Introduction

Previous research on Fe-C-Al-Mn self-shielded arc steel welds that focused on inclusion formation and solidification microstructure [1, 2] showed that aluminum nitride inclusions formed first from the liquid, followed by δ -ferrite. This microstructural evolution was successfully predicted by computational thermodynamic and kinetic models. The focus of current ongoing work is to extrapolate the above models to nonequilibrium conditions that are experienced at high solid-liquid interface velocities.

Kurz and co-workers [3, 4, 5, 6] have considered the transitions from equilibrium to nonequilibrium solidification as a function of liquid-solid interface velocities. Their work has shown that with increasing liquid solid interface velocity, (i) elemental partitioning ($k_V = \text{solid composition/liquid composition}$) at a velocity “V” increases from the equilibrium value (k_{eq}) and reaches unity at high velocities; $k_{eq} < k_V < 1$, (ii) primary solidification of a nonequilibrium phase may occur and (iii) liquid-solid interface morphology changes from planar to cellular to dendritic and back to planar. In some steel welds, mixed bands of ferrite and austenite may also occur. It is noteworthy that all of these phenomena are interrelated. It is indeed possible to model these effects in binary alloys and higher order multicomponent alloys using dendritic solidification and interface response function theories [3–11]. Nonequilibrium phase selection during weld solidification in stainless steel welds has been studied in detail by others [see cited references 12 to 27 in 12]. These researchers have shown that by increasing the liquid-solid interface velocity, a transition from equilibrium δ -ferrite to δ -austenite solidification in stainless steels can be forced. In all these studies, the experimental proof for such transitions was attained by post weld characterization. This was possible since the solidification microstructure

[†] Research sponsored by the U.S. Department of Energy, Division of Materials Sciences and Engineering under contract Number DE-AC05-00OR22725 with UT-Battelle, LLC

was not destroyed during weld cooling. In low alloys steels, post-weld characterizations of weld do not yield conclusive evidence for such transitions due to the destruction of the solidification microstructure by solid-state transformations. Usually, the rapid cooling conditions that lead to nonequilibrium austenite solidification in low alloy steels also leads to rapid decomposition of austenite to martensite. As a result, after noticing the martensite formation in the fusion zone, one cannot distinguish the actual transformation route taken by the low alloy steel between the following two possible routes given: (I) Liquid \rightarrow Partitionless α -ferrite \rightarrow massive austenite formation \rightarrow displacive transformation to martensite or (II) Liquid \rightarrow nonequilibrium austenite formation \rightarrow displacive transformation to martensite.

With in-situ characterization techniques [13, 14, 15], one can track these changes as a function of solidification conditions. In recent study, a transition from equilibrium α -ferrite solidification to nonequilibrium α -austenite solidification was observed in an Fe – 0.234C – 0.50 Mn – 1.70 Al – (wt.%) steel weld with an increase in weld cooling rate [12] was monitored using time-resolved X-ray diffraction technique (TRXRD). The phase diagram for this composition showed that the equilibrium primary solidification should occur by the formation of α -ferrite. The TRXRD results from a slowly cooled weld showed the formation of α -ferrite first from the liquid. In contrast, the rapidly cooled welds showed the formation of nonequilibrium austenite. The present paper presents recent results obtained from Fe-C-Al-Mn system with high aluminum concentrations in excess of 3 wt.%. The focus of this research is to study whether similar nonequilibrium phase selection can occur with large concentrations of aluminum, the ferrite stabilizer.

Experimental

A flux-cored arc weld with Fe - 0.28 C - 0.45 Mn - 0.39 Si – 3.7 Al - 0.004 Ti - 0.003 O - 0.035 N (wt.%) composition was deposited as an overlay on a normal C-Mn steel bar. The aluminum concentrations in these deposits are higher than that (1.7 wt.%) used in the previous research [12]. Stationary GTAW (Gas Tungsten Arc Welding) ‘spot’ welds were made on these weld overlay surfaces by striking an arc on a stationary bar and then terminating this arc after the weld pool had achieved its maximum diameter or after a certain hold time. Three types of experiments were performed in this investigation. (1) The first experiment simulated an arc-strike phenomenon, by melting and solidifying within one second on the surface of the sample under the tungsten electrode. (2) Similar to previous work [12] rapid cooling rates were achieved by extinction of the arc after a hold time of 17 second. (3) The arc current was reduced slowly and allowed to extinguish itself after the current drops below a critical value. In this later condition, the measurement location was chosen very close to a critical distance at which a rapid increase in liquid-solid interface velocity occurs due to arc extinction at low arc currents. Therefore, the results will correspond to a condition where a transition from equilibrium to nonequilibrium solidification may occur if it all possible. In-situ TRXRD measurements were performed during spot welding using the 31-pole wiggler beam line, BL 10-2 at the Stanford Synchrotron Radiation Laboratory. The reader is referred to a previous publication for the details on experimental set up [12].

Results and Discussion

Experimental Results

TRXRD results from all three experiments are shown in Fig. 1. The corresponding micrographs are shown in Fig 2. In experiment 1, the welding arc was on for 1 second and the measurements were made very close to the center of weld. The measurements show [see Fig. 1a] the presence of the bcc (110) diffraction peak at room temperature. Within a fraction of

second of arc-strike, the bcc diffraction peaks move to low 2θ values, indicating a rapid lattice expansion. Subsequent to that diffraction information was lost, indicating liquid formation. As soon as the arc was extinguished, the measurements showed the appearance of bcc (110) diffraction and indicated that the primary solidification phase is δ -ferrite. Subsequently, the position of this peak moved to higher 2θ values indicating the lattice contraction due to weld cooling.

It is important to note that experiment 1 produces a small weld, which restricts the range of interface velocities that is possible during rapid cooling conditions of a spot weld [16]. The optical microstructure from the FZ in this condition [see Fig. 2a] shows finely spaced columnar δ -ferrite grains. Since the arc-on time was 1 second, the HAZ microstructure did not change much from its original condition. The original base metal microstructure also had a columnar δ -ferrite morphology since it was prepared by a cladding operation. Interestingly, one can notice the decrease in dendrite arm spacing across the fusion line boundary.

Results from experiment 2 also show the primary solidification phase to be δ -ferrite as indicated by the presence of bcc (200) diffraction peaks [see Fig.1b]. It is important to note that for a similar condition, in another Fe-C-Al-Mn steel containing less aluminum (1.7 wt.%), a transition from equilibrium δ -ferrite to austenite solidification occurred [12]. Fig. 1b also shows the formation of the fcc (220) diffraction peaks after the formation of the bcc (200) peak, presumably in the final stages of solidification. The intensity of this austenite peak decreases during further

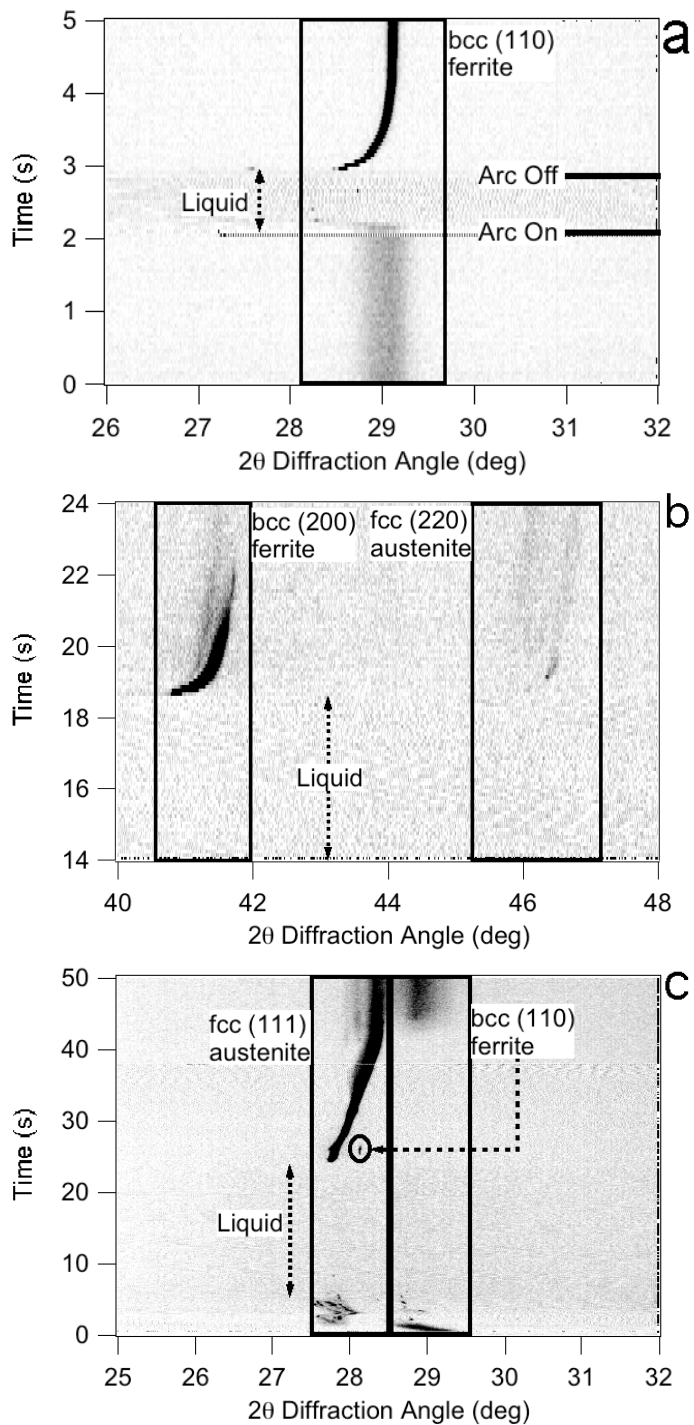


Fig. 1. TRXRD results are shown in an image format. The horizontal axis is the diffraction angle and indicates which phases exist while the vertical axis is the time. The diffraction peaks appear with darker contrast and the background intensity with lighter contrast. (a) Results from experiment 1 show the formation of δ -ferrite from liquid. (b) Results from experiment 2 show the primary solidification of δ -ferrite (c) Results from experiment 3 showing the primary solidification of austenite.

cooling, presumably due to the decomposition at low temperature. The optical microstructure from the FZ region in this condition [see Fig. 2b] shows columnar δ -ferrite grains similar to the results from experiment 1; however, the spacing is a little higher than that of experiment 1. This may be attributed to changes in temperature gradient and liquid solid interface velocity. Since the arc-on time was higher than experiment 1, the HAZ region in experiment 2 contains coarse δ -ferrite and intragranular austenite regions. Results from experiment 3 show that the primary solidification phase to be austenite as indicated by the appearance of fcc (111) diffraction peak much before the bcc (110) diffraction peaks. It is noteworthy that the measurement location is very close to a region where the interface velocity increased rapidly. This suggests that even in the presence of a high aluminum concentration (a ferrite stabilizer), there is a transition from equilibrium δ -ferrite to austenite with an increase in liquid-solid interface velocity. The optical microstructure from this condition is in agreement with the above result [see Fig. 2c]. Very close to the HAZ region, the primary solidification occurs by δ -ferrite as shown by the presence of the columnar dendritic microstructure. But with an increase in distance from the boundary, some instability in the dendritic microstructure was observed [marked by arrow in Fig. 2c] and eventual replacement by martensitic microstructure. TRXRD results indicate that this martensitic microstructure forms from nonequilibrium austenite. Similar observations were made in the previous work [12].

Thermodynamic and Interface Response Function Calculations

A calculated cross section of phase diagram predicted for the present steel and weld composition, using ThermoCalc® [17] with solid solution database [18], is shown in Fig. 3a. The calculations show that in equilibrium the primary solidification phase must be δ -ferrite. This prediction is in agreement with results from experiments 1 and 2. The results from experiment 3 are not in agreement with

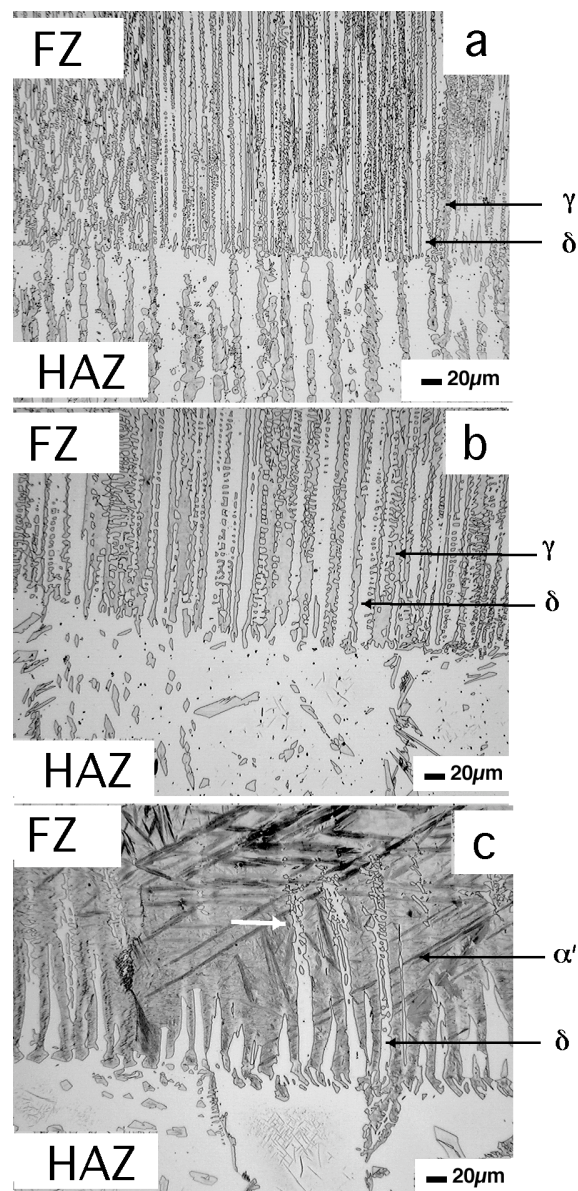


Fig. Optical microstructures at heat-affected-zone (HAZ) - fusion zone (FZ) boundary from all three experiments are compared. (a) Results from experiment 1 show the presence of columnar δ -ferrite (white regions) and interdendritic transformed austenite (darkly etching) in the FZ. (b) Results from experiment 2 show the presence of coarse δ -ferrite in HAZ and columnar δ -ferrite in the FZ (c) Results from experiment 3 show the presence of δ -ferrite dendrites close to the boundary, however, but a martensitic microstructure (darkly etching) can be observed a short distance into the FZ.

the phase diagram because austenitic solidification is far from equilibrium. To evaluate this transition, the interface response function theories developed by Kurz and co-workers [3–6] were used. Thermodynamic information needed for the calculations were obtained from ThermoCalc® [17] with solid solution database. The results are shown in Fig. 3b. The calculations using published [4–6] Gibbs Thompson coefficients (Γ) show that the transition from δ -ferrite to austenite is impossible in this alloy, i.e., the liquid-ferrite interface temperature is always higher than that of liquid-austenite for all interface velocities. Additional calculations considered the sensitivity of the interface response function analysis to different parameters. While keeping the Γ for austenite constant, the Γ for ferrite was varied. The results that by increasing Γ for ferrite by only two orders of magnitude the liquid-ferrite interface temperature can be reduced below that of liquid-austenite above a critical velocity of 1×10^{-3} m/s. This calculation agrees with the experimentally observed ferrite solidification at low interface velocity and the formation of austenite at high interface velocities. Nevertheless, further theoretical work is necessary to justify the selection of Gibbs Thompson coefficients for ferrite and austenite in steels containing both interstitial and substitutional elements.

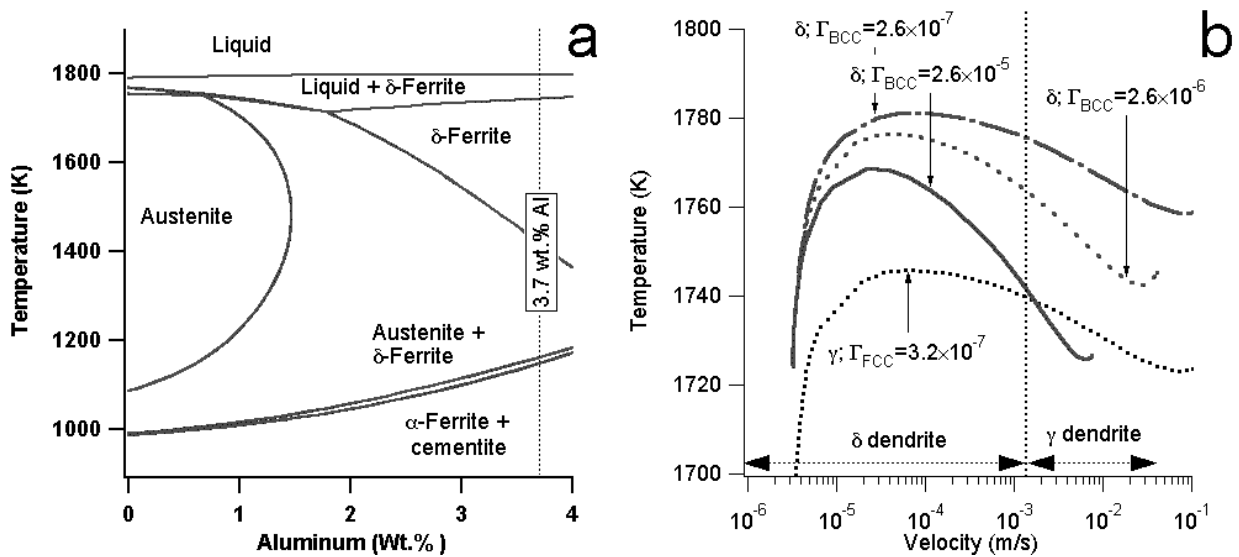


Fig. 3. (a) Cross section of a phase diagram for Fe-0.28 wt.% C – 0.5 wt.% Mn – Al system shows that a weld with 3.7 wt.% aluminum should solidify first as δ -ferrite. The interface response function theory calculations of liquid-ferrite and liquid-austenite dendrite tip temperatures as a function of interface velocity. The plots also show the result of changing the Gibbs Thompson coefficient (Γ) on the liquid-ferrite dendrite tip temperature.

Conclusions

The phase selection phenomenon in an Fe-0.2C-0.5Mn-3.7Al (wt.%) self-shielded flux cored arc weld metal deposits was evaluated with TRXRD technique using synchrotron radiation. The changes in liquid-solid interface velocities were produced by changes in the arc welding conditions. At low interface velocities, primary solidification occurred by δ -ferrite, which is in agreement with thermodynamic calculations. The results show that, above a critical interface velocity, a shift was induced in the primary solidification mode from equilibrium δ -ferrite to nonequilibrium austenite. Using the theoretical treatment of dendritic solidification and phase selection maps advanced by Kurz and with modified thermodynamic parameters, the above transition was successfully described.

Acknowledgements

This research was sponsored by the U.S. Department of Energy, Division of Materials Sciences and Engineering under contract No. DE-AC05-00OR22725 with UT-Battelle, LLC. A portion of this work was performed under the auspices of the U. S. Department of Energy, Lawrence Livermore National Laboratory, under Contract No. W-7405-ENG-48. The authors thank Drs. O. Barabash and M. Muruganath of ORNL for helpful comments on the manuscript.

References

1. S. S. Babu, S. A. David, and M. A. Quintana, "Modeling microstructure evolution in self-shielded flux cored arc welds," *Welding Journal*, **80** (2001), 91s-97s
2. M. A. Quintana, J. McLane, S. S. Babu, S. A. David, "Inclusion formation in self shielded flux-cored arc welds," *Welding Journal*, **80** (2001) 98s-105s
3. W. Kurz, B. Giovanola and R. Trivedi, "Theory of microstructural development during rapid solidification," *Acta Metall*, **34** (1986) 823-830
4. S. Fukumoto and W. Kurz, "The δ to γ transition in Fe-Cr-Ni alloys during laser treatment," *ISIJ International*, **37** (1997) 677-684
5. S. Fukumoto and W. Kurz, "Prediction of the δ to γ transition in austenitic alloys during laser treatment," *ISIJ International*, **38** (1998) 71-77
6. S. Fukumoto and W. Kurz, "Solidification phase and microstructure selection maps for Fe-Cr-Ni alloys," *ISIJ International*, **39** (1999) 1270-1279
7. W. Kurz and D. J. Fisher: Fundamentals of Solidification, Fourth Revised Edition, Trans Tech Publications Ltd, USA, 1998, Page 242.
8. W. J. Boettinger, S. R. Coriel, A. L. Greer, A. Karma, M. Rappaz, and R. Trivedi, "Solidification microstructures: Recent developments, future directions," *Acta Mater.*, **48** (2000) 43-70.
9. R. Trivedi, and W. Kurz, "Dendritic Growth," *International Materials Reviews*, **39** (1994), 49-74
10. O. Hunziker, M. Vandyoussefi, and W. Kurz, "Phase and microstructure selection in peritectic alloys close to the limit of constitutional undercooling," *Acta Mater*, **46** (1998) 6325-6336.
11. M. J. Aziz, "Model for solute redistribution during rapid solidification," *J. Appl. Physics*, **53** (1982) 1158-1168
12. S. S. Babu, J. W. Elmer, J. M. Vitek, and S. A. David, "Time-resolved X-ray diffraction investigation of primary weld solidification in Fe-C-Al-Mn steel welds," *Acta Mater*, **50** (2002) 4763-4781
13. S. A. Moir and D. M. Herlach, "Observation of phase selection from dendrite growth in undercooled Fe-Ni-Cr melts," *Acta Mater*, **45** (1997) 2827-2837
14. C. B. Arnold, M. J. Aziz, M. Schwarz, and D. M. Herlach, "Parameter-free test of alloy dendrite-growth theory," *Physical Reviews B*, **59** (1999), 334-343
15. J. W. Elmer, J. Wong, and T. Ressler, "In-situ observations of phase transformations during solidification and cooling of austenitic stainless steel welds using time-resolved X-ray diffraction," *Scripta Mater.*, **43** (2000), 751-757
16. W. Zhang, G. G. Roy, J. W. Elmer and T. DebRoy, "Modeling of heat transfer and fluid flow during gas tungsten arc spot welding of low carbon steel," *J. Applied Physics*, **93** (2003), 3022-3033
17. B. Sundman, B. Jansson, and J. O. Andersson, "The thermo-calc databank system," *Calphad*, **9** (1985), 1-153.
18. SGTE Solution Database (1992) Editor: B. Sundman, Division of Computational Thermodynamics, Royal Institute of Technology, Stockholm, Sweden.